Northumbria Research Link

Northumbria
University
NEWCASTLE

University**Library**

Integrated label-free erbium-doped fiber laser biosensing system for detection of single cell *Staphylococcus aureus*

Jiandong Liu [a], Bin Liu [a,**], Juan Liu [a], Xing-Dao He [a], Jinhui Yuan [c], Zabih Ghassemlooy [b], Hamdi Torun [b], Yong-Qing Fu [b], Xuewu Dai [b], Wai Pang Ng [b], Richard Binns [b], Qiang Wu [a,b,*]

[a] *Key Laboratory of Opto-Electronic Information Science and Technology of Jiangxi Province, Nanchang Hangkong University, Nanchang, 330063, China*
[b] *Optical Communications Research Group. Faculty of Engineering and Environment, Northumbria University, Newcastle Upon Tyne, NE1 8ST, United Kingdom*
[c] *Research Center for Convergence Networks and Ubiquitous Services, University of Science & Technology Beijing, Beijing, 100083, China*

ABSTRACT

A critical challenge to realize ultra-high sensitivity with optical fiber interferometers for label free biosensing is to achieve high quality factors (Q-factor) in liquid. In this work a high Q-factor of 10^5, which significantly improves the detection resolution is described based on a structure of single mode -core-only -single mode fiber (SCS) with its multimode (or Mach-Zehnder) interference effect as a filter that is integrated into an erbium-doped fiber laser (EDFL) system for excitation. In the case study, the section of core-only fiber is functionalized with porcine immunoglobulin G (IgG) antibodies, which could selectively bind to bacterial pathogen of *Staphylococcus aureus* (*S. aureus*). The developed microfiber-based biosensing platform called SCS-based EDFL biosensors can effectively detect concentrations of *S. aureus* from 10 to 10^5 CFU/mL, with a responsivity of 0.426 nm wavelength shift in the measured spectrum for *S. aureus* concentration of 10 CFU/mL. The limit of detection (LoD) is estimated as 7.3 CFU/mL based on the measurement of *S. aureus* with minimum concentration of 10 CFU/mL. In addition, when a lower concentration of 1 CFU/mL is applied to the biosensor, a wavelength shift of 0.12 nm is observed in 10% of samples (1/10), indicating actual LoD of 1 CFU/mL for the proposed biosensor. Attributed to its good sensitivity, stability, reproducibility and specificity, the proposed EDFL based biosensing platform has great potentials for diagnostics.

1. Introduction

The World Health Organization (WHO) has reported that foodborne diseases are among the highest morbidity and mortality worldwide and pose a major threaten to social and economic development [1]. The main cause of foodborne illness is the pathogenic bacteria including Staphylococcus aureus (*S. aureus*) *S. aureus* produces toxins and invasive enzymes, and exists widely in nature. It can produce several types of protein-based enterotoxins that cause acute gastroenteritis [2]. Enterotoxin can withstand boiling temperature (100 °C) for 30 min without being destroyed and can easily cause food poisoning in people by showing symptoms of vomiting and diarrhea [2]. *S. aureus* poses risks during food processing, storage, transportation, and sales, leading to severe food poisoning. To effectively prevent diseases caused by

foodborne pathogenic bacteria and ensure food safety, rapid and effective detection methods are urgently required. Traditional culture-based detection methods, such as agar dilution, breakpoint or disk diffusion, need at least 24 h to culture the sample, thus not suitable for rapid detection [3]. Several new detection methods have emerged including electrochemical biosensor [4,5], fluorescence sensor [6], impedance biosensors [7,8], surface-enhanced Raman spectroscopy (SERS), etc [9, 10]. However, they are mostly confined to the laboratory environments and commonly lack of reusability [11].

Previously Majumdar et al. [12] proposed electrochemical amperometric biosensors that quantifies changes in *S. aureus* concentration with a limit of detection (LoD) 10 CFU/mL and a good linearity between concentration and current output. However, these electrochemical biosensors are often prone to false current measurements due to ambient

---

fluctuations.

In recent years, many researchers have been working on fiber-based biosensors, which have advantages of anti-electromagnetic interference and easy manufacturing capability [13,14]. Fiber biosensors based on surface plasmon resonance (SPR) [15], tapered optical fiber [16,17], U-bent fiber [18], long-period grating [19], and fiber Bragg grating [20] have shown fast and highly sensitive responses to bacteria, but their manufacturing processes are often complex and costly. In contrast, fiber optic interference structures are becoming more popular as biosensors.

Biosensors based on Machzender interference (MZI) structures have been widely studied and developed owing to their low cost, simple structure, and moderate sensitivity [16]. In 2017, Li et al. proposed to form an MZI interference structure by controlling the waist diameter of conical multimode fiber, and to detect *Escherichia coli* by modifying a biofilm reaction layer on the surface of the interference structure with a LoD of 10^3 CFU/mL [21]. In 2020, Kaushik et al. proposed the use of a photosensitive (PS) fiber optic MZI structure for the measurement of collagen in the human body [22]. In 2022, Wang et al. proposed a lateral offset spliced coreless fiber MZI biosensor for cytokine tumor necrosis factor-α (TNF-α) detection [23]. However, biosensors based on MZI is not yet regarded as a practical solution, which is mainly due to the difficulty of analyzing its multi-stripe transmission spectrum. One possible option for simplifying the MZI-based sensors would be to integrate the single mode – core only – single mode (SCS) structure within the fiber laser cavity. The interferometric feature of MZI structures allows selection of wavelength (λ) in the fiber laser cavity, i.e., an output with a single wavelength with a high signal-to-noise ratio, thus simplifying the spectral assessment with an enhanced detection resolution [24]. There are many examples, such as deployment of singlemode-multimode-singlemode (SMS) structures in fiber laser cavities [24,25]. For example, in Ref. [26], a biosensing platform based on the tapered fiber integrated in fiber laser system was reported as a molecular biosensor in a case study where avidin molecules with varying concentrations were measured. The fiber laser system is able to achieve a single-wavelength output, thus simplifying sensor's output and analysis [26].

In the conventional optical fiber sensing systems, broadband light sources (BLSs) or amplified spontaneous emission (ASE) are often used, which have a large full-width half maximum (FWHM) in the optical spectrum and a low optical signal-to-noise ratio (OSNR) in the available wavelength range [27]. Therefore, the application of these conventional systems for concentration detection of biomolecules is limited to a great extent. In this paper, to overcome the difficulty of analyzing multi-stripe transmission spectrum and improve detection resolution, SCS-based EDFL biosensors is proposed by introducing multimode interference structures based on SCS functionalized by porcine IgG into an EDFL. Experimental result demonstrates that the SCS-based EDFL biosensors achieves a single-wavelength output with high Q factor of 10^5. Its full-width at half-maximum (FWHM) and OSNR values are 0.12 nm and 41.2 **dB**, respectively. The verified LoD of SCS-based EDFL biosensors for detecting *S. aureus* is 1 CFU/mL.

2. Materials and methods

A schematic diagram of the proposed SCS structure is illustrated in Fig. 1(a), which is constructed using two single-mode fibers (SMFs, G652D, Yangtze Optical Fibre and Cable, China) and a small diameter core-only fiber (COF, CL-1010-C, Yangtze Optical Fibre and Cable, China). A commercial welding machine (Fujikura 80C, FUJIKURA, Japan) is used to fuse the ends of COF (2 cm long and 62.5 μm of diameter) with the SMFs. Fig. 1(b) shows a microscope image (GP-660 V) of fusion spliced SMF and COF under optical magnification of 4.5 ×, a working distance 95 mm, and an electrical magnification of 135 ×. The injection of light from the SMF output into the COF excites the multimode interference effect. This interference mode will interact with the surrounding medium by formation of an evanescent field. A slight change in the surrounding medium alters the transmission modes of the COF, thus resulting in a significant wavelength shift in the interference spectrum, which can be readily measured using a spectrum analyzer [28].

The sensing head is obtained by functionalizing the SCS structure. We choose the porcine immunoglobulin G (IgG) antibody (product code: b1108, purchased from BEIJING BERSEE SCIENCE AND TECHNOLOGY CO. LTD), which is specifically bound to *S. aureus* [30–33]. The detailed processes of functionalization are listed as follows:

  i. The SCS structure is immersed for 4 h in a silane solution (3-(3-triethoxysilylpropyl) oxolane-2,5-dione) (product code:
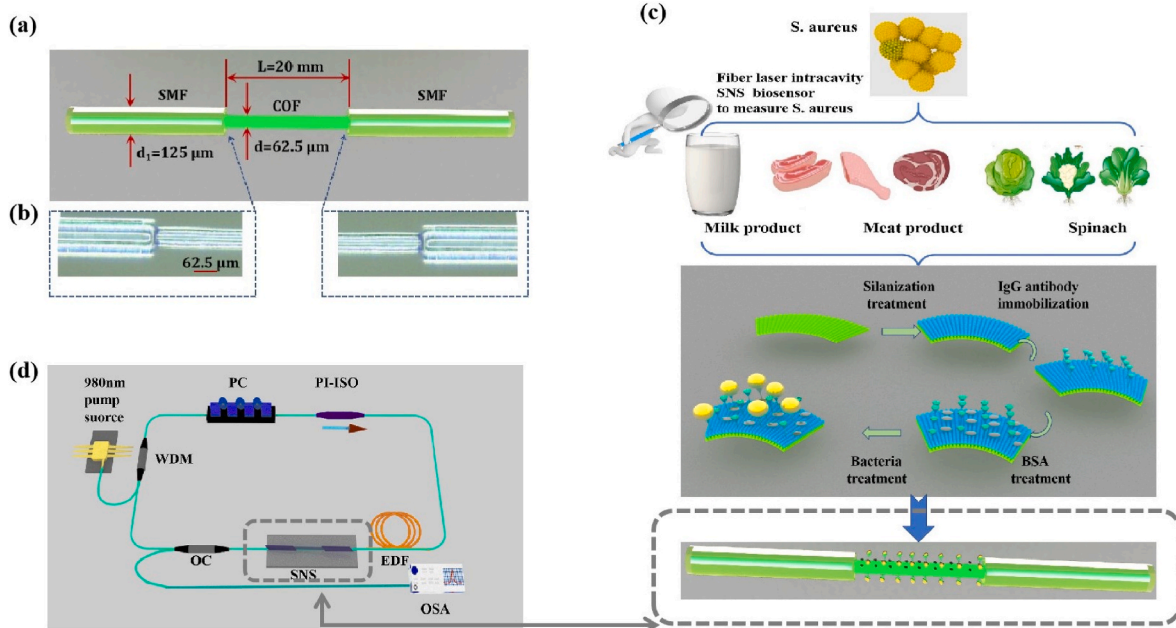

Fig. 1. (a) Schematic diagram of SCS structure, (b) micrograph of SCS structure. SMF: single mode fiber; COF: core-only fiber, (c)schematic diagram of SCS structure functionalization process, and (d)diagram of SCS-based EDFL biosensors experiment device.

T195932-5 g, purchased from aladdin) diluted to 5% with the anhydrous ethanol solution, which forms carboxyl groups on the surface of the fiber.

   ii. The SCS structure is cleaned twice using a buffer solution (pH = 6, product code: P118681, purchased from aladdin), after which it is immersed in a freshly prepared activation reagent for 30 min. The activation reagent is composed of hydroxy-2, 5-Dioxopyroli-dine-3-Sulfonicacid sodium salt (NHSS, product code: H109337, purchased from Sinopharm Chemical Reagent Co., Ltd) and 1-(3-dimethylaminopropyl) -3-ethylcar-Bodiimide hydrochloride (EDC, product code: 39141134, purchased from aladdin), mixed in a buffer solution (pH = 6).

   iii. The SCS structure is washed with the phosphate buffered saline (PBS, product code: SH30256.01, with a pH value of 7.4, purchased from GE Healthcare Life Sciences). It is then immersed into solution of porcine IgG antibodies, which is fixed onto surfaces of fiber optic sensor after it is soaked in the solution for 4 h.

   iv. The SCS structure is cleaned three times with the PBS, and then immersed into a solution diluted with the PBS to 1% bovine serum albumin (BSA, product code: A119741, purchased from aladdin). The purpose of this is to block the remaining carboxyl groups that do not bind to porcine IgG antibodies. This will prevent non-specific binding, in which non-target biomolecules bind directly to the carboxyl group.

Fig. 1(c) shows the functionalization process of the fiber's surface, including the above mentioned four key steps.

In order to solve the difficulties to analyze the transmission spectrum generated from the sensing process and improve the measurement accuracy, an EDFL is used to interrogate the transmission spectrum of the sensing head. The specific structure of SCS-based EDFL biosensors experimental device is shown in Fig. 1(d). Using a wavelength division multiplexer (WDM, WDM-1X2-980/1550–2, BOKAI GUANGDIAN, China) coupler, a 980 nm pump source (VLSS-980-B-650-FA, CONNET, China) is connected to the ring cavity of laser. The common port of the WDM coupler is passed through a polarization controller (PC, 3-Paddle Fiber Polarization Controller, BOKAI GUANGDIAN, China), which is used to adjust polarization state. To ensure the unidirectional propagation of the light, we use a polarization independent isolator (PI–ISO, Polarization Insensitive Isolator, BOKAI GUANGDIAN, China). The PI-ISO outputs are then applied to an erbium-doped fiber (EDF, 5 m long, 8/125, Nufern) amplifier and the SCS interference structure, the latter of which plays the role of a sensing head. The output of SCS is injected to a WDM coupler then to an optical spectrum analyzer (OSA, MS9710C, Anritsu, Japan) via a 90:10 optical coupler (OC, WIC-1X2-1550-10/90-0-A40, BOKAI GUANGDIAN, China).

Numerical simulation of the SCS structure is firstly performed using the mode propagation method [24,25]. The parameters of both SMF and COF used in the numerical simulation are listed in Table 1. Fig. 2(a) shows the transmission optical field distribution of the SCS structure along the *x-z* direction at a wavelength of 1550 nm in air. Optical field evolutions (in *x-y* direction) can be clearly demonstrated in the transmission process of the COF section, due to the modes' interference along the length of COF. The result shows that the SCS structure is sensitive to change of surrounding environment.

Fig. 2(b) shows spectral responses of SCS structure with various refractive indices (RIs) of 1, 1.33, 1.34, and 1.35. Results of interference wavelength vs. different RIs are shown in Fig. 2(c), which reveals a

sensitive redshift with the increasing RI, and the obtained sensitivity is ~201 nm/RIU (refractive index unit).

3. Experimental results and discussion

3.1. Refractive index sensitivity of SCS-based EDFL biosensor

Fig. 3(a) compares the laser spectrum (black line) output from the SCS-based EDFL biosensor with the transmission spectrum (red line) of a single SCS fiber structure. The FWHM of the output laser spectrum reaches ~0.12 nm, whereas the OSNR value and Q-factor exceed 40 **dB** and 10^5, respectively. At the same time, the detection resolution of the sensor is defined as [29]:

$$R = 3\sigma = 3\sqrt{\sigma_{ampl-noise}^2 + \sigma_{spect-res}^2 + \sigma_{temp-induced}^2} \tag{1}$$

$$\sigma_{ample-noise} = (FWHM) / \left(4.5 \times \left(OSNR^{0.25}\right)\right) \tag{2}$$

$$\sigma_{spect-res} = R_w / 2\sqrt{3} \tag{3}$$

$$\sigma_{temp-induced} = 10^{-5} \text{ nm} \tag{4}$$

where $\sigma_{ampl-noise}$, $\sigma_{spect-res}$, and $\sigma_{temp-induced}$ are the spectral resolution, thermal variation of the system, and amplitude noise, respectively. Combining Eqs. (1)–(4), the sensor's detection resolution is calculated as 7.65 and 0.054 nm, respectively, before and after introducing the EDFL. In the calculation process, the OSNR values are 9.8 **dB** and 41.2 **dB**, and R_w values, which represent the scanning resolutions of OSA, are 0.2 and 0.05 before and after the introduction of EDFL, respectively. The results clearly show that the detection resolution of the sensor is significantly improved, translating into a much lower LoD. In addition, the interferometric effect of SCS structures with its filtering functionality has led to SCS-based EDFL biosensor generating a single λ and eliminate the difficulty of analyzing multi-stripe transmission spectrum

The influence of temperature on SCS-based EDFL biosensor is studied and discussed. The experimental results are shown in Fig. 3(b). When the temperature increases from 36 °C to 72 °C, the wavelength of the output spectrum of the sensor shifts from 1558.03 nm to 1557.2 nm, and the sensitivity is −0.02 nm/^{0}C. The results show that temperature has a limited effect on the measurement accuracy due to our tests were carried out at room temperature within 30 min, and the temperature variation is very small (<1 °C). The refractive index (RI) sensitivity of SCS-based EDFL biosensor is measured. Fig. 3(c) shows wavelength shifts vs. RI, where the wavelength shift increases with the increases of RI value, illustrating a monotonical red-shift. Fig. 3(d) shows the spectrum of a typical SCS fiber structure with a 2 cm long COF. After several measurements, the RI sensitivity of the sensor is 200.86 nm/RIU, and the maximum error bar is 0.09, which agrees very well with the simulation result as shown in Fig. 2(c). Therefore, we chose the SCS structure with a 2 cm COF as the sensing head, functionalized the SCS structure and immobilized antibodies, and introduced EDFL to construct an SCS-based EDFL biosensor for further experimental measurement of *S. aureus*.

3.2. SCS-based EDFL biosensor for detection of S. aureus

The functionalized SCS-based EDFL biosensors can be used to measure the *S. aureus*. The measurement steps are listed as follows:

   A. The SCS structure is functionalized using porcine IgG antibodies with three different concentrations of 50, 100, and 200 μg/mL, respectively. A total of 45 functionalized SCS structures are made, and each antibody concentration are associated with 15 SCS structures.

   B. SCS-based EDFL biosensors functionalized by 50 μg/mL antibody are then selected for the following sensing process.

Table 1
Parameters of fibers used in the numerical simulation.

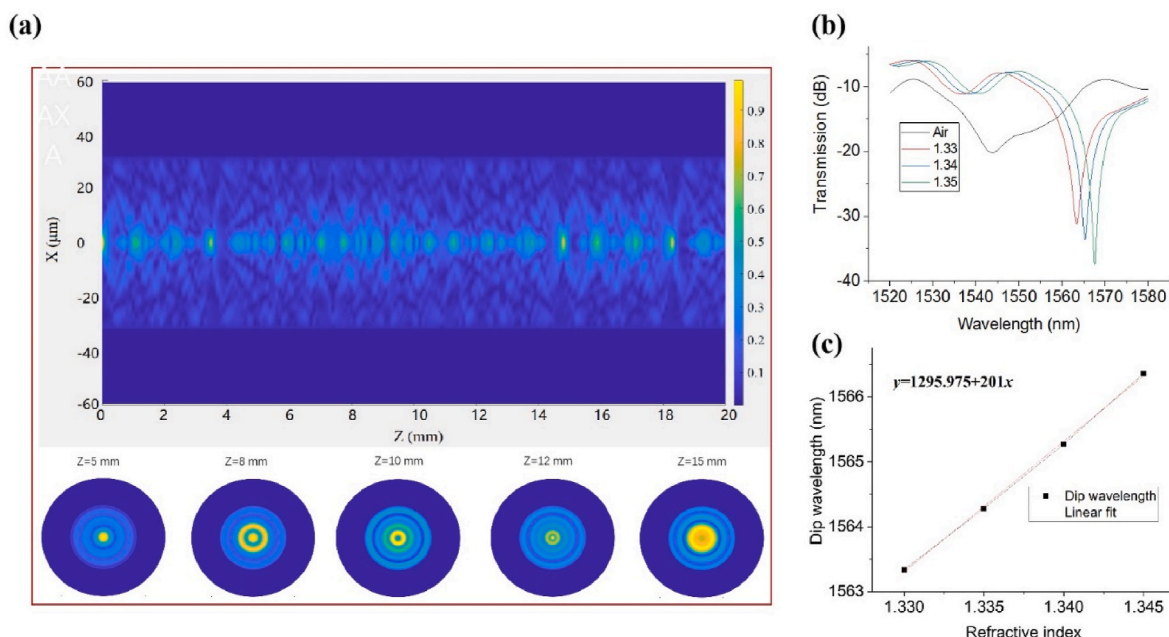| Fiber type	Core diameter (μm)	cladding diameter (μm)	RI of core	RI of cladding
SMF	8	125	1.4507	1.4428
COF	62.5	120	1.444	1–1.365

Fig. 2. Simulated results of the SCS structure: (a) optical field distribution along x-z direction at λ of 1550 nm and mode field distributions of cross sections of a COF of a range length of 5, 8, 10, 12, and 15 mm, (b) the transmission spectra for RI of 1, 1.33, 1.34, and 1.35, and (c) wavelength vs. the refractive index.
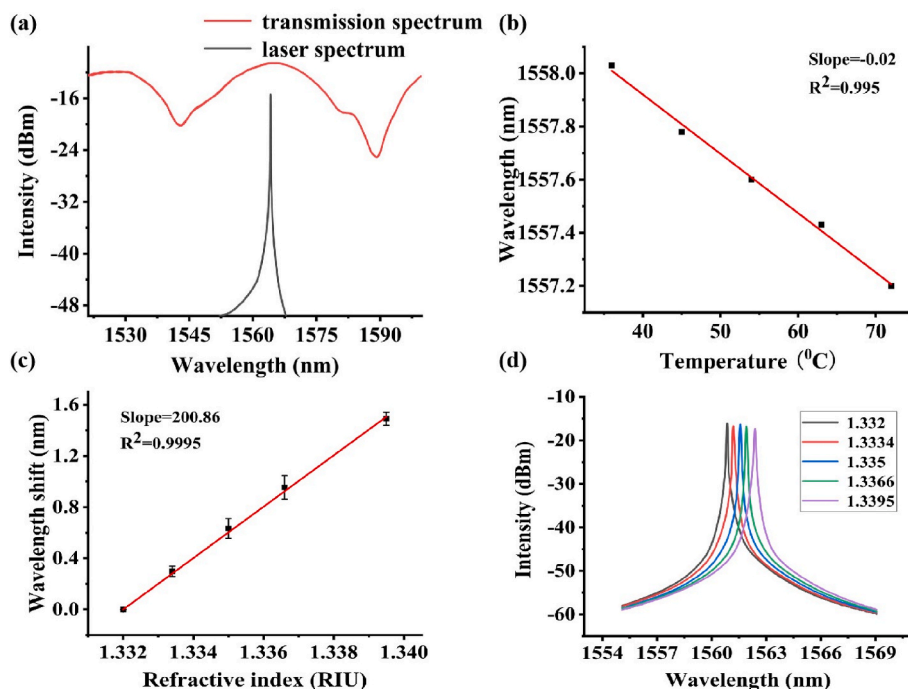

Fig. 3. (a) Comparison of the laser spectra (black lines) from the output of an SCS EDFL biosensor with the transmission spectra (red lines) from a single SCS fiber structure, (b) Linear fitting diagram of the variation of wavelength with temperatures, (c) Linear fitting diagram of the variation of wavelength shift with refractive index, and (d) spectrum of SCS fiber structure with a 2 cm long COF.

   i. The SCS-based EDFL biosensor is immersed in the PBS solution for 30 min to stabilize the integrated sensing platform.

  ii. The SCS-based EDFL biosensor is immersed into a sample of *S. aureus* (10 CFU/mL), and SCS-based EDFL biosensors are then used to monitor the specific recognition of antigens and antibodies.

 iii. Three same SCS-based EDFL biosensors are used to repeat the above steps for proving the repeatability.

 iv. The concentrations of *S. aureus* samples are then changed to 10^2, 10^3, 10^4 and 10^5 CFU/mL, respectively, and then the steps (i), (ii) and (iii) are repeated for each concentration.

C. SCS-based EDFL biosensors functionalized with the 100 μg/mL antibody are selected to repeat step B.

D. SCS-based EDFL biosensors functionalized by 200 μg/mL antibody are selected to repeat step B.

The bonding of porcine IgG antibodies with *S. aureus* effectively

changes the RI value and thickness of the media around the SCS structure, thus resulting in shifts of the spectral wavelengths for the SCS-based EDFL biosensor. Fig. 4(a) and (b) show images (obtained using the scanning electron microscope, SEM) of the functionalized SCS-based EDFL biosensor bound with *S. aureus*. It should be noted that the *S. aureus* bound to the SCS structure conforms to the biological characteristics of *S. aureus*, which is spherical in shape and between 0.5 and 1.5 μm in size.

The SCS-based EDFL biosensor which is functionalized using porcine IgG antibody (200 μg/mL) is then immersed into the solution of *S. aureus* (10^3 CFU/mL), and the obtained spectral responses of SCS-based EDFL biosensor are illustrated in Fig. 5(a). Different concentrations of *S. aureus* samples (i.e., 10, 10^2, 10^3, 10^4, and 10^5 CFU/mL) are used to study effect of *S. aureus*' concentration on performance of SCS-based EDFL biosensors. Five SCS-based EDFL biosensor (fabricated under the same conditions) are functionalized using porcine IgG antibody (200 μg/mL) for detecting *S. aureus* samples. Fig. 5(b) depicts the wavelength shifts as a function of time for these five SCS-based EDFL sensors immersed into *S. aureus* solution with various concentration. To study the effect of porcine IgG concentration on SCS-based EDFL biosensors, three SCS-based EDFL biosensors are functionalized with antibodies with different concentration (50, 100, and 200 μg/mL), respectively. The SCS-based EDFL biosensor is then immersed in a solution of *S. aureus* (10^3 CFU/mL). Fig. 5(c) shows the results of wavelength shifts for three SCS-based EDFL biosensors immersed in the same sample of *S. aureus*.

Results shown in both Fig. 5(b) and (c) indicate that the wavelength shifts of the SCS-based EDFL biosensor occur in the first 20 min, revealing that the binding of *S. aureus* to porcine IgG antibody on the surface of the functional SCS-based EDFL biosensors occurs in this period. During the surface-specific binding of *S. aureus* to the SCS-based EDFL biosensor, the data of wavelength shifts and the immersion time show an exponential relationship, and these results are consistent with the reported dynamics of immune behavior [37]. Fig. 5(b) also show that testing in a higher *S. aureus* concentration results in a significantly increased wavelength shift when the SCS-based EDFL biosensor is functionalized by the porcine IgG antibody (200 μg/mL). The reason is that the SCS-based EDFL biosensor is more likely to capture *S. aureus* in a high concentration solution. At the same *S. aureus*' concentration (10^3 CFU/mL) the wavelength shifts of SCS-based EDFL biosensor treated with much higher concentration of porcine IgG antibody shows significantly increased value. This is because the binding sites for *S. aureus* increase with the concentration of antibody. When the concentration of antibody used modify the surfaced of fiber biosensor is 200 μg/mL, the maximum value of wavelength change is ~1.005 nm. Fig. 5(b) and (c) show that the maximum wavelength shift in PBS solution for 30 min is ±0.03 nm.

Reproducibility of the SCS-based EDFL biosensors is demonstrated by testing 45 SCS structures separated into three groups, with each group functionalized with the porcine IgG antibody concentrations of 50, 100, and 200 μg/mL, respectively. Each group is then separated into

five sub-groups, to be bound with *S. aureus* with their concentrations of 10, 10^2, 10^3, 10^4, and 10^5 CFU/mL, respectively.

Fig. 6(a) depicts the wavelength shifts as a function of *S. aureus* concentration for three different porcine IgG antibodies. The SCS-based EDFL biosensor show wavelength shifts of {0.289, 0.618, 0.711, 0.757, 0.787}; {0.346, 0.7423, 0.937, 0.985, 1.015}; and {0.426, 0.858, 1.019, 1.155, and 1.34} nm, which are obtained using various *S. aureus*' concentrations of 10, 10^2, 10^3, 10^4, and 10^5 CFU/mL. The maximum error bar can be achieved with the lowest concentration of 10 CFU/mL. One possible reason for this is that *S. aureus* tends to be more evenly distributed in higher concentrations than those in lower concentrations.

Twelve SCS structure functionalized with the porcine IgG antibody (50 μg/mL) are prepared to further study the specificity of the SCS-based EDFL biosensors. Firstly, four identical SCS-based EDFL biosensors are immersed into four different analytes, namely 10^2 CFU/mL *S. aureus*, 10 mg/mL BSA, 3.95×10^7 CFU/mL *E. coli* and 8.7×10^4 CFU/mL Salmonella, respectively. Secondly, the processes are repeated three times with the SCS-based EDFL biosensors. Fig. 6(b) shows the obtained experimental results, where wavelength shifts for the identical SCS-based EDFL biosensors are 0.64, 0.045, 0.069, and 0.062 nm for *S. aureus*, BSA, *E. coli*, and Salmonella, respectively. Obviously, SCS-based EDFL biosensor has a specific selectivity for *S. aureus*, which is attributed to its specific combination of antigen and antibody.

The calibration curves of the fiber biosensor are obtained as shown in Fig. 6(c), where a linear regression function is obtained, which is $y = 0.23 \log[x \, (\text{CFU}/\text{mL})] + 0.29$ (slope = 0.23), with a correlation coefficient of 0.93. According to LoD equation [38]:

$$\text{LoD} = 3.3 \frac{S_y}{a} \qquad (5)$$

$$s_y = \sqrt{\frac{\sum (y_i - \bar{y})^2}{degrees \ of \ freedom}} \qquad (6)$$

where LoD is detection limit; S_y denotes the standard deviation of responses for around expected LoD and a is the slope of a linear calibration line. When the calibration law is semilogarithmic, the LoD equation needs to be redefined as follows:

$$\text{LoD} = 3.3 \times \frac{2.303 S_y x}{\frac{dy}{d\log_{10}^x}} \qquad (7)$$

In Fig. 6(c), the value of x is 10 CFU/mL, $\frac{dy}{d\log x} = 0.23$. S_y is 0.022 calculated at the minimum concentration 10 CFU/mL, thus the LoD is estimated as 7.3 CFU/mL.

We then experimentally investigate the detection effect of this SCS-based EDFL biosensor at a concentration *S. aureus* of 1 CFU/mL. The volume of the sample used in each test is about 1 mL. For the *S. aureus* sample (1 CFU/mL), the number of *S. aureus* bacterium is 1 CFU on average in each test. Furthermore, the number of bacteria in the extracted sample can only be an integral number. Therefore, due to the
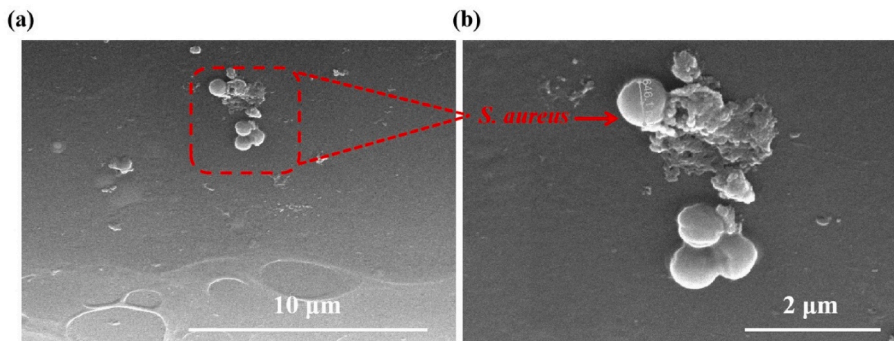

Fig. 4. SEM images of the functional SCS-based EDFL biosensor bound with *S. aureus* with different scale bar: (a) 10, and (b) 2 μm.
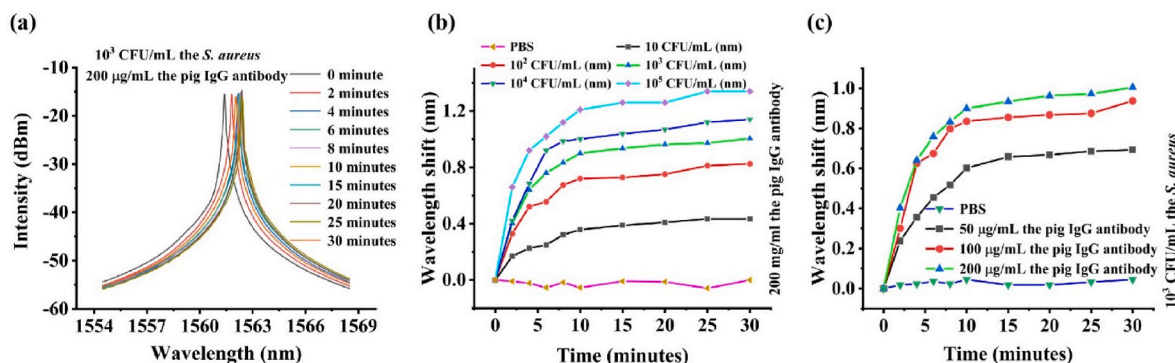
Fig. 5. (a) Spectral responses of the SCS-based EDFL biosensors treated with 200 μg/mL porcine IgG antibody for detecting 103 CFU/mL *S. aureus* solution concentration, (b) measured wavelength change at different concentrations of *S. aureus* samples (10, 102, 103, 104, and 105 CFU/mL), and (c) different IgG antibody concentrations (50, 100, and 200 μg/mL) for detecting *S. aureus*.
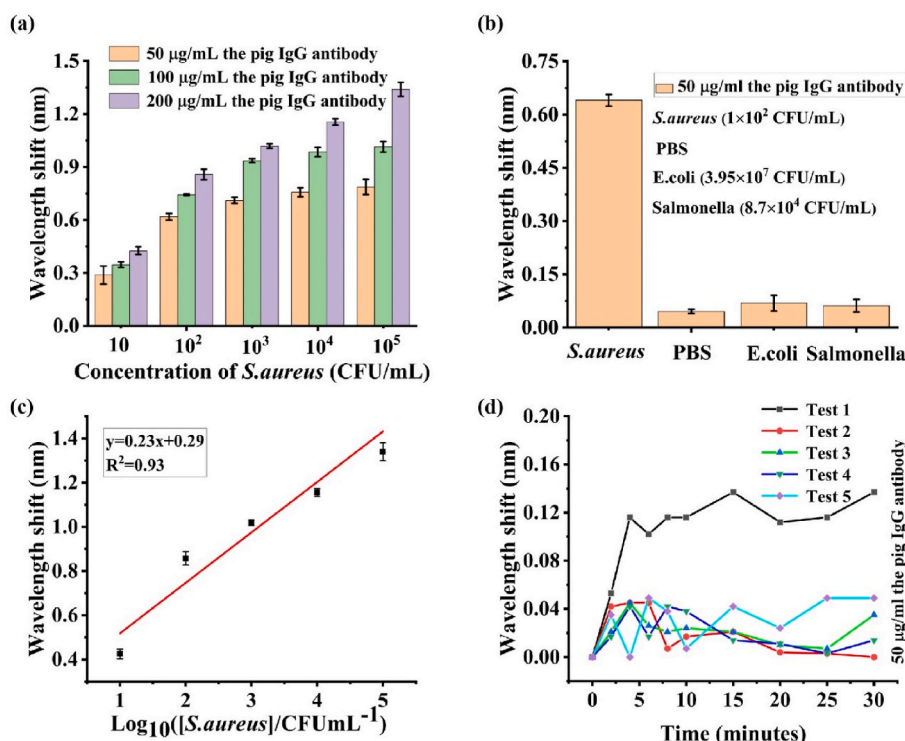

Fig. 6. (a) Reproducibility of SCS-based EDFL biosensor, (b) specificity results of SCS-based EDFL biosensor, (c)measured wavelength shift of the SCS-based EDFL biosensor at solutions with different concentrations of *S. aureus*, and (d) under concentration of 1 CFU/mL with multiple tests.

probability issue, the actual concentration of each sample could be varied significantly, which could be 0, 1, or 2 CFU/mL, etc. However, it should be noted that if the actual number of bacteria in the samples is taken as zero, it would be impossible for the fiber-optic sensor to capture any *S. aureus*. Even with one or two bacteria in the testing sample, the probability of capturing one or two *S. aureus* bacteria in the sample slot is low, because the SCS structure has a small diameter of 62.5 μm and the chance of bacteria being captured by the antibody immobilized on the SCS is low.

From the analysis results at the limiting concentration, the SCS-based EDFL biosensor which is treated with the porcine IgG antibody (50 μg/mL) can be applied to test the responses with the limiting concentration of 1 CFU/mL. Ten repeatable experiments are conducted under the same conditions. The conditions mentioned here are the same SCS-based EDFL biosensor, treated with porcine IgG antibody (50 μg/mL), measured at a concentration of 1 CFU/mL *S. aureus* sample at room temperature. The sample solution was changed and washed with PBS for each

measurement, but the volume (1.0 mL) and concentration (1.0 CFU/mL) remain unchanged. Only in one of 10 test results, a significant spectral response (wavelength shift of 0.12 nm) is obtained using the SCS-based EDFL biosensor. Fig. 6(d) shows the comparisons the one case which shows the significant spectral response, and with the other four cases without showing apparent responses. The change in the laser wavelength in other tests is less than ±0.03 nm, which is similar to the response of PBS solution, thus indicating that the SCS-based EDFL biosensor does not capture *S. aureus*. It should be noted that the theoretical LoD is 7.3 CFU/mL, calculated using a semi-logarithmic relationship. Based on our experimental testing, the developed sensor was able to detect 1 CFU/mL *S. aureus* sample.

Table 2 summarizes the sensing concentration achieved from the newly proposed SCS-based EDFL biosensor in this study, together with those of optical sensing platforms reported in literature. It is clear to see that the actual minimum measured value of the SCS-based EDFL biosensor is relatively low, compared to those reported in literature,

Table 2

A summary of biosensing used for the detection of *S. aureus*.

Methods	Actually minimum measured concentration	Reference
Electrochemical aptasensor based on gold/nitrogen-dopedcarbon nano-onions	10 CFU/mL	[34] (2021)
Electrochemiluminescent biosensor utilizing the binding between immunoglobulin G and protein A	3×10^3 CFU/mL	[35] (2016)
Fluorescence detection base on CdSe quantum dots coupled with bacteria	10^2 CFU/mL	[36] (2009)
Surface-enhanced Raman scattering (SERS) biosensor	10 CFU/mL	[9] (2009)
Long-period fiber grating (LPFG) sensor (IgY)	100 CFU/mL	[19] (2021)
Tapered SNSFC biosensor	70 CFU/mL	[31] (2020)
SCS-based EDFL biosensor	**1.0 CFU/mL**	**This paper**

demonstrating the excellent performance of the new sensing platform.

4. Conclusions

In summary, a biofunctionalized SCS structure was integrated into EDFL for ultra-high sensitive detection of *S. aureus* and then its effectiveness is experimentally demonstrated. The SCS structure as a filter, which was prepared by fusing a section of COF with a diameter of 62.5 μm between two SMFs, achieves the EDFL spectrum with a high Q factor of 10^5. In a case study, the SCS structure treated with the porcine IgG antibody. This antibody has its specificity to bind with *S. aureus*. The performance of SCS-based EDFL biosensor with different concentrations of porcine IgG antibodies was reported. The SCS-based EDFL biosensor functionalized with the 200 μg/mL porcine IgG antibody has a better sensitivity than those with 50 and 100 μg/mL antibodies. The average wavelength shift reached 0.426 nm for detection of 10 CFU/mL *S. aureus*. Furthermore, the SCS-based EDFL biosensors demonstrated a good stability by immersing the PBS solution for 30 min, and the maximum wavelength shift detected was ±0.03 nm. Finally, the probability for detection of limit concentration *S. aureus* (1 CFU/mL) was discussed and demonstrated with repeated experiments. The SCS-based EDFL biosensor simplify the outputs and analysis of the sensor and improved the measured minimum concentrations of the fiber biosensor, and therefore are appropriate for practical applications.

Author Contributions

Jiandong Liu: Investigation, Formal analysis, Writing – original draft, Investigation; Bin Liu: Conceptualization, Funding acquisition, Supervision, Formal analysis, Writing – original draft, Methodology, Writing – review & editing; Juan Liu: Formal analysis, Writing – review & editing; Xingdao He: Supervision, Formal analysis, Writing – review & editing; Jinhui Yuan: Formal analysis, Writing – review & editing; Zabih Ghassemlooy: Formal analysis, Writing – review & editing; Hamdi Torun: Formal analysis, Writing – review & editing; Yong-Qing Fu: Formal analysis, Writing – review & editing; Xuewu Dai: Formal analysis, Writing – review & editing; Wai Pang Ng: Formal analysis, Writing – review & editing; Richard Binns: Formal analysis, Writing – review & editing; Qiang Wu: Conceptualization, Supervision, Funding acquisition, Formal analysis, Methodology, Writing – review & editing.

Declaration of competing interest

The authors declare that they have no known competing financial interests or personal relationships that could have appeared to influence the work reported in this paper.

Data availability

No data was used for the research described in the article.

References

[1] Momna Rubab, Hafiz Muhammad Shahbaz, Amin N. Olaimat, Deog-Hwan Oh, Biosensors for Rapid and Sensitive Detection of Staphylococcus aureus in Food, Biosensors & Bioelectronics, 2011, pp. 49–57, https://doi.org/10.1016/j.bios.2018.01.023.

[2] Hennekinne Jacques-Antoine, Marie-Laure De Buyser, Sylviane Dragacci, Staphylococcus aureus and its food poisoning toxins: characterization and outbreak investigation, FEMS (Fed. Eur. Microbiol. Soc.) Microbiol. Rev. 36 (2016) 815–836, https://doi.org/10.1111/j.1574-6976.2011.00311.x.

[3] Hatice Ceylan Koydemir, Haluk Külah, Canan Özgen, Alpaslan Alp, MEMS biosensors for detection of methicillin resistant Staphylococcus aureus, Biosens. Bioelectron. 29 (2011) 1–12, https://doi.org/10.1016/j.bios.2011.07.071.

[4] Yi Wu, Hui Chai, Development of an electrochemical biosensor for rapid detection of foodborne pathogenic bacteria, Int. J. Electrochem. Sci. 12 (2017) 4291–4300, h10.20964/2017.05.09.

[5] Jyoti Bhardwaj, Sivaranjani Devarakonda, Suveen Kumar, Jaesung Jang, Development of a paper-based electrochemical immunosensor using an antibody-single walled carbon nanotubes bio-conjugate modified electrode for label-free detection of foodborne pathogens, Sensor. Actuator. B Chem. 253 (2017) 115–123, https://doi.org/10.1016/j.snb.2017.06.108.

[6] Tinging Miao, Zhouping Wang, Shuang Li, Xin Wang, Sensitive fluorescent detection of Staphylococcus aureus using nanogold linked CdTe nanocrystals as signal amplification labels, Microchim. Acta 172 (2011) 431–437, https://doi.org/10.1007/s00604-010-0505-z.

[7] Preeti Pathania, Arunima Sharma, Binod Kumar, Praveen Rishi, C. Raman Suri, Selective identification of specific aptamers for the detection of non-typhoidal salmonellosis in an apta-impedimetric sensing format, Microchim. Acta 184 (2017) 1499–1508, https://doi.org/10.1007/s00604-017-2098-2.

[8] Amjed Abdullah, Ibrahim Jasim, Mohammed Alalem, Majed Dweik, Mahmoud Almasri, MEMS based impedance biosensor for rapid detection of low concentrations of foodborne pathogens, in: 2017 IEEE 30th International Conference on Micro Electro Mechanical Systems (MEMS), Las Vegas, NV, USA, 2017, pp. 381–385, https://doi.org/10.1109/MEMSYS.2017.7863421.

[9] Junfeng Wang, Xuezhong Wu, Chongwen Wang, et al., Magnetically assisted surface-enhanced Raman spectroscopy for the detection of Staphylococcus aureus based on aptamer recognition, ACS Appl. Mater. Interfaces 7 (2009) 20919, https://doi.org/10.1021/acsami.5b06446.

[10] Hui Zhang, Xiaoyuan Ma, Ying Liu, et al., Gold nanoparticles enhanced SERS aptasensor for the simultaneous detection of Salmonella typhimurium and Staphylococcus aureus, Biosens. Bioelectron. 74 (2015) 872–877, https://doi.org/10.1016/j.bios.2015.07.033.

[11] Pooja Devi, Anupma Thakur, Shweta Chopra, , et al.Praveen Kumar, et al., Ultrasensitive and selective sensing of selenium using nitrogen-rich ligand interfaced carbon quantum dots, ACS Appl. Mater. Interfaces 9 (2017) 13448–13456, https://doi.org/10.1021/acsami.7b00991.

[12] Tania Majumdar, Runu Chakraborty, Utpal Raychaudhuri, Praveen Kumar, et al., Development of PEI-GA modified antibody based sensor for the detection of S. aureus in food samples, Food Biosci. 4 (2013) 38–45, https://doi.org/10.1016/j.fbio.2013.08.002.

[13] Ling Chen, Bin Liu, Juan Liu, et al., Novel microfiber sensor and its biosensing application for detection of hCG based on a singlemode-tapered hollow core-singlemode fiber structure, IEEE Sensor. J. (2020), https://doi.org/10.1109/JSEN.2020.2986327.

[14] Rahul Kumar, Yuankui Leng, Bin Liu, et al., Ultrasensitive biosensor based on magnetic microspheres enhanced microfiber interferometer, Biosens. Bioelectron. 145 (2019), 111563, https://doi.org/10.1016/j.bios.2019.111563.

[15] Siddharth Kaushik, Umesh K. Tiwari, Sudipta S. Pal, Ravindra K. Sinha, Praveen Kumar, et al., Rapid detection of Escherichia coli using fiber optic surface plasmon resonance immunosensor based on biofunctionalized Molybdenum disulfide (MoS2) nanosheets, Biosens. Bioelectron. 126 (2018) 49–57, https://doi.org/10.1016/j.bios.2018.11.006.

[16] M.A. Mustapa, M.H. Abu Bakar, Y. Mustapha Kamil, et al., Bio-functionalized tapered multimode fiber coated with dengue virus NS1 glycoprotein for label free detection of anti-dengue virus NS1 IgG antibody, IEEE Sensor. J. (2018) 1, https://doi.org/10.1109/JSEN.2018.2813352, 1.

[17] Angela Leung, Kishan Rijal, P. Mohana Shankar, Mutharasan Raj, Effects of geometry on transmission and sensing potential of tapered fiber sensors, Biosens. Bioelectron. 21 (2006). ±02–2209. 10.1016/j.bios.2005.11.022.

[18] Reshma Bharadwaj, V.V.R. Sai, Kamini Thakare, , et al.Praveen Kumar, et al., Evanescent wave absorbance based fiber optic biosensor for label-free detection of E. coli at 280nm wavelength, Biosens. Bioelectron. 26 (2011) 3367–3370, https://doi.org/10.1016/j.bios.2010.12.014.

[19] Wenbo Gan, Zhenli Xu, Yaowei Li, Praveen Kumar, et al., Rapid and sensitive detection of Staphylococcus aureus by using a long-period fiber grating immunosensor coated with egg yolk antibody, Biosens. Bioelectron. 199 (2022), https://doi.org/10.1016/j.bios.2021.113860.

[20] Rajesh Srinivasan, Sharath Umesh, Swetha Murali, Sundarrajan Asokan, Sai Siva Gorthi, Bare fiber Bragg grating immunosensor for real-time detection of Escherichia coli bacteria, Biophotonics 10 (2017) 224–230, https://doi.org/10.1002/jbio.201500208.

[21] Yanpeng Li, HuiMa, Lin Gan, et al., Immobilized optical fiber microprobe for selective and sensitive Escherichia coli detection, J. Biophot. 24 (2017), https://doi.org/10.1002/jbio.201700162.

[22] Brajesh Kumar Kaushik, Lokendra Singh, Ragini Singh, et al., Detection of collagen-IV using highly reflective metal nanoparticles—immobilized photosensitive optical fiber-based MZI structure, IEEE Trans. NanoBioscience 19 (2020) 477–484, https://doi.org/10.1109/TNB.2020.2998520.

[23] Bo Wang, Shaoxiang Duan, Hao Zhang, et al., A label-free lateral offset spliced coreless fiber MZI biosensor based on hydrophobin HGFI for TNF-α detection, Optoelectron. Lett. 18 (2022), https://doi.org/10.1007/s11801-022-2061-2.

[24] Qiang Wu, Yuwei Qu, Juan Liu, et al., Singlemode-multimode-singlemode fiber structures for sensing applications – a review, IEEE Sensor. J. 21 (2021) 12734–12751, https://doi.org/10.1109/JSEN.2020.3039912.

[25] Qiang Wu, Yuliya Semenova, Pengfei Wang, Gerald Farrell, High sensitivity SMS fiber structure based refractometer – analysis and experiment, Opt Express 19 (2011) 7937–7944, https://doi.org/10.1016/j.bios.2021.113860.

[26] M. Mansora, M.H. Abu Bakar, M.A. Mahdir, et al., Taper biosensor in fiber ring laser cavity for protein detection, Opt Laser. Technol. 125 (2020), 106033, https://doi.org/10.1016/j.optlastec.2019.106033.

[27] Chunran Sun, Muguang Wang, Jingxuan Liu, Ye Shen, Linjun Liang, Shuisheng Jian, Fiber ring cavity laser based on modal interference for curvature sensing, IEEE Photon. Technol. Lett. 28 (2016) 1, https://doi.org/10.1109/LPT.2016.2517666, 1.

[28] Ling Chen, Yuan-Kui Leng, Bin Liu, et al., Ultrahigh-sensitivity label-free optical fiber biosensor based on a tapered singlemode- no core-singlemode coupler for Staphylococcus aureus detection, Sensor. Actuator. B Chem. 320 (2020), 128283, https://doi.org/10.1016/j.snb.2020.128283.

[29] Cai Lu, Yong Zhaoa, Xue-gang Li, A fiber ring cavity laser sensor for refractive index and temperature measurement with core-offset modal interferometer as tunable filter, Sensor. Actuator. B Chem. 242 (2017) 673–678, https://doi.org/10.1016/j.snb.2016.11.112.

[30] Johann Deisenhofer, Crystallographic refinement and atomic models of a human Fc fragment and its complex with fragment B of protein A from Staphylococcus aureus at 2.9- and 2.8-A resolution, Biochemistry 20 (1981) 2361–2370, https://doi.org/10.1021/bi00512a001.

[31] Weijun Kong, Jie Xiong, Huan Yue, Zhifeng Fu, Sandwich fluorimetric method for specific detection of Staphylococcus aureus based on antibiotic-affinity strategy, Anal. Chem. 87 (2015) 9864–9868, https://doi.org/10.1021/acs.analchem.5b02301.

[32] Hongfei Gao, Shijia Yang, Jing Han, et al., Double-site recognition of pathogenic bacterial whole cells based on an antibiotic-affinity strategy, Chem. Commun. 51 (2015) 12497–12500, https://doi.org/10.1039/c5cc02814k.

[33] Xiangyu Meng, Guotai Yang, Fulai Li, Taobo Liang, Weihua Lai, Hengyi Xu, Sensitive detection of Staphylococcus aureus with vancomycin-conjugated magnetic beads as enrichment carriers combined with flow cytometry, ACS Appl. Mater. Interfaces (2017), https://doi.org/10.1021/acsami.7b05479.

[34] Esmail Sohouli, Masoumeh Ghalkhani, Tahereh Zargar, Praveen Kumar, et al., A new electrochemical aptasensor based on gold/nitrogen-doped carbon nano-onions for the detection of Staphylococcus aureus, Electrochim. Acta 403 (2022), 139633, https://doi.org/10.1016/j.electacta.2021.139633.

[35] Huan Yue, Yali Zhou, Pingshi Wang, et al., A facile label-free electrochemiluminescent biosensor for specific detection of Staphylococcus aureus utilizing the binding between immunoglobulin G and protein A, Talanta 153 (2016) 401–406, https://doi.org/10.1016/j.talanta.2016.03.043.

[36] Xiuheng Xue, Jian Pan, Huiming Xie, Juhua Wang, Shuang Zhang, Fluorescence detection of total count of Escherichia coli and Staphylococcus aureus on water-soluble CdSe quantum dots coupled with bacteria, Talanta 77 (2009) 1808, https://doi.org/10.1016/j.talanta.2008.10.025, 1803.

[37] Guigen Liu, Kaiwei Li, Micro/nano optical fibers for label-free detection of abrin with high sensitivity, Sensor. Actuator. B Chem. 215 (2015) 146–151, https://doi.org/10.1016/j.snb.2015.03.056.

[38] Yuzuru Hayashi, Rieko Matsuda, I.T.O. Katsutoshi, et al., Detection limit estimated from slope of calibration curve: an application to competitive ELISA, Anal. Sci. 21 (2005) 167–169, https://doi.org/10.2116/analsci.21.167.